

AN INVESTIGATION OF METHODS OF ESTIMATING CRACK DRIVING FORCE FOR DEFECTS IN OR NEAR WELDS

M C Smith¹, M R Goldthorpe², P J Bouchard¹ and P Prottey³

¹ British Energy Generation Ltd, Barnett Way, Barnwood, Gloucester, GL4 3RS, UK

² M R Goldthorpe Associates, The Grange, 2 Park Vale Road, Macclesfield, SK11 8AR, UK

³ W S Atkins Science and Technology, 220 Aztec West, Park Avenue, Almondsbury, Bristol, BS32 4SY, UK

ABSTRACT:

In recent years considerable effort has been invested in advanced computational methods for estimating the residual stresses developed in multi-pass welds. Such stresses are then often used in defect assessments. The simplified methods for treating residual stresses embodied in defect assessment procedures such as R6 are usually validated by comparison with cracked-body finite element analysis.

A recent series of studies performed as part of the development programme for R6 considered the combination of yield magnitude residual stresses, a primary load, and yield magnitude thermal stresses. Two geometries were considered: a cylinder containing an external circumferential crack, and a sphere containing an internal axi-symmetric defect. The J-integral due to the combined loading history was obtained by cracked body finite element analysis.

It was found that the value obtained for the J-integral depends on the methods used to introduce the defect into the structure. Three methods were employed: a pre-existing defect; a defect that is introduced after formation of the residual stresses by simultaneous release of the crack flank nodes; and a defect that is allowed to grow by progressive release of crack flank nodes.

The implications of these results for the assessment of defects in welds are discussed. In particular, it is noted that the value predicted for the J-integral depends on the time of formation of the defect.

INTRODUCTION

The sentencing of defects at welds is a common task for defect assessment procedures such as R6 [1], BS7910 [2], or the recently developed SINTAP procedure [3]. Defects at welds are often subjected to a combination of primary stresses due to system pressure or external loads, secondary stresses due to thermal loading, and weld residual stress. In some cases, both the thermal and residual stresses may be individually of yield magnitude [4]. The defect assessment procedure must be able to make an estimate of crack driving force that is conservative, but not overly so. This problem naturally divides into two parts: first making an estimate of the residual stress-strain field in the vicinity of the weld; and then using that estimate to calculate the crack driving force.

Residual stresses may be estimated by direct measurement, by the use of published compendia [3], or by finite element simulations of the welding process. Finite element techniques in particular have received

considerable attention in recent years (for example, see [5]), and allow the evaluation of both the stress field and the strain history in the vicinity of a postulated defect. In contrast, direct measurement and the use of compendia only yield an estimate of the residual stress field.

Welding residual stress fields are normally handled in defect assessment procedures such as R6 [1] by treating them as elastic. Thus the welding strain history at the defect location is ignored, and an elastic stress intensity factor calculated from the elastic-plastic residual stresses in the plane of the defect in an uncracked body. R6 incorporates methods for handling the plasticity effects of primary and secondary loads alone, and the interaction between primary and secondary loads [1, 6], but in common with other assessment procedures, does not take account of any effect the welding stress-strain and crack development history have on the crack driving force generated by the residual stress field. This is a pragmatic approach, since in most, if not all, real plant assessments the strain history is unknown, and the best that can be hoped for is a good estimate of the residual stress field. However it may not always be reasonable.

The simplified assessment methods embodied in a procedure such as R6 are normally validated against both the behaviour of real defects in small-scale and large-scale fracture tests (for example, see [7, 8]), and the results of non-linear cracked-body finite element analyses. In the latter, the J-integral [9] is evaluated directly, and compared with estimates made using R6 [1]. Cracked-body finite element analysis is relatively straightforward for externally applied loads such as pressure, dead-weight or thermal shock, and combinations thereof. However the addition of weld residual stresses raises a number of issues, which include:

- The validity of the J-integral as a characterising parameter. Does the stress and strain history local to the crack tip after formation of the defect allow a valid, path-independent calculation of J?
- The time of formation of the defect. Is the defect present during the welding process (for example a lack of fusion defect or shrinkage cracking in a multi-pass weld), or does it form after welding is complete and the residual stress/strain field has developed fully?

Strictly, the characterisation of crack tip fields by J is based on non-linear elastic materials where the strain energy is fully recoverable and is a unique function of the strain field [9]. This characterisation also applies to inelastic materials provided that the loading is 'proportional'. In practice this means that there is no unloading of the cracked region, so that the recoverable strain energy is still approximately a unique function of strain. In these circumstances, any imposed system of loads on a cracked body will produce a singular stress field at the crack tip whose intensity is controlled by a single parameter J. In such elastic-plastic analyses the J-integral is path-independent and can be determined by integrating over any domain surrounding the crack tip. This limitation makes it unlikely that a valid value of J could be obtained from a non-linear cracked-body finite element analysis that performs a full simulation of the welding process with a defect that forms close to or within the weld early in the welding process. The complex cyclic stress-strain history in the weld region will violate the assumption of proportional loading. Thus simulations of pre-existing defects must use a representation of the residual stress-strain field that allows a valid calculation of J.

The postulated time of formation of a defect may have an important influence on the crack driving force induced by a residual stress-strain field. If the defect is assumed to be pre-existing and stationary, then the crack tip region will respond to the entire imposed stress/strain history. If the defect is assumed to have formed after welding, or to have advanced in service by some sub-critical mechanism, then the residual stress-strain history will have much less effect.

In this paper, the effect of the mode of formation of a defect in a residual stress-strain field is examined in two geometries: a thick-walled cylinder containing an external circumferential defect, and a spherical shell containing an internal defect at a repair weld. The cylinder is loaded by a residual stress field and then a through-wall thermal gradient, while the sphere is loaded by a residual stress field, followed by internal pressure and a through-wall thermal gradient. Three methods are used to introduce a crack into the finite element meshes, and their effect on the predicted value of the J-integral examined:

1. the defect is always present;
2. the defect is introduced after formation of the residual stress field, by simultaneous release of all the crack face nodes;

- the defect is introduced after formation of the residual stress field, by progressive release of the crack face nodes, starting at the surface of the component and ending at the final crack tip.

ANALYSIS

Circumferentially cracked cylinder

These analyses are fully reported elsewhere [10, 11], and only a brief description is given here¹. The ABAQUS [12] finite element mesh is shown in Figure 1, and models a thick-walled cylinder of mean radius to thickness ratio $R_m/t=5$, containing an external fully-circumferential defect of normalised depth $a/t=0.2$. The material was an austenitic steel with a 0.2% offset stress, $\sigma_{0.2}$, of 290.4 MPa.

The loading consisted of a simulated “residual” stress field, followed by an additional thermal load. Two methods were used to impose the residual stress field. In the first, a high initial temperature distribution was specified in a block of material on the outside surface adjacent to the crack. The final temperature of the entire mesh was set to 20°C, and an elastic-plastic analysis performed to determine the resultant residual stresses and strains. In the second, an initial radial temperature distribution was applied to the entire cylinder in the stress free state, the final temperature of the mesh again set to 20°C, and an elastic-plastic analysis performed to determine the resultant residual stresses and strains. The resulting axial stress distributions are shown in Figure 2. Both methods produce a through-wall bend type of stress distribution, but Method 2 produces a much more intense stress-strain field, with yield over 40% of the section compared with a crack depth of 20%. The subsequent thermal load was imposed as an exponential radial temperature change [10]. Eight different through-wall temperature distributions were applied, and these developed peak elastic thermal stresses which varied from $0.8\times\sigma_{0.2}$ to over $4\times\sigma_{0.2}$ [10].

The defect was assumed either to be pre-existing, or to have formed by simultaneous release of all the crack face nodes over a single ABAQUS load step after imposition of the residual stress field and before application of the thermal load. The combination of defect introduction method and loading was expected to cause unloading in the mesh along the crack flanks, and potentially elsewhere in the mesh remote from the crack tip. Because of this a very fine crack tip mesh was used, since close to the crack tip the effect of local unloading of material becomes less significant compared with the intense singular fields of stress and strain which arise from the ‘remote’ fields of stress. A very fine finite element mesh is thus required [13] to determine path-independent results for J in such situations where there is non-proportional loading or unloading of the crack tip. In the current study, J was evaluated over twenty contours near the crack tip.

Spherical shell

These analyses are also reported elsewhere [4] so only a brief description of the relevant details is given. The geometry was based upon that of a pressurised water reactor primary loop coolant pump, of internal radius 1016 mm and wall thickness 191 mm, containing a repair weld, shown in Figure 3. The repair weld was assumed to contain the axi-symmetric “ring” defect of various depths, as also shown in Figure 3. Details of the very fine crack tip region of the ABAQUS [12] axi-symmetric mesh are shown in Figure 4. Two materials assumptions were used: all weld metal with $\sigma_{0.2}=338$ MPa at the operating temperature of 290°C, and mixed weld metal and casting material, the latter with $\sigma_{0.2}=146$ MPa [4].

The loading consisted of the residual stress field (applied using the same approach as Method 1 above), followed by internal pressure and a through-wall temperature distribution. The uncracked-body elastic stresses in the plane of the defect are shown in Figure 5.

In these analyses no attempt was made to model a pre-existing defect. Instead, the defect was assumed to form after imposition of the residual stress field. Two methods were used to introduce the crack: “simultaneous” opening and “progressive” opening (see above). In general, the crack was introduced prior to imposition of the pressure or thermal loads. However some studies were performed on a crack that was opened progressively after application of the pressure load. A range of crack depths was examined.

¹ The analyses reported in [11] cover the effect of primary load in addition to residual and thermal loads. They are not discussed further here.

RESULTS

Circumferentially cracked cylinder

Figure 6 plots the ratio of the effective stress intensity factor, $K_J = \sqrt{EJ/(1-\nu^2)}$, for a defect introduced after imposition of the residual stress field to that for a pre-existing defect, as a function of the secondary reference stress ratio R (this is a measure of the severity of the secondary loading, and is defined in the Appendix). It can be seen that the effective stress intensity factor ratio is less than one for residual stress alone, and for residual stress followed by the less severe thermal loads, and rises towards one for very high levels of the subsequent thermal load. The predicted crack driving force is thus higher for a pre-existing defect. The effect is more marked for the more severe residual stress distribution. This is not a surprising result, since the pre-existing defect responds both to the elastic residual stress field and the plastic strains generated during its imposition, while the defect introduced afterwards responds only to the elastic residual stress and strain field. The rise in the effective stress intensity factor ratio towards unity as the severity of the subsequent thermal load increases is also as expected. Both the residual and thermal loads are secondary in nature and are effectively self-limiting since they are strain-controlled. Thus as greater amounts of plasticity are associated with the thermal load alone, so the prior residual load becomes less important.

Figure 7 compares simple elastic stress intensity factors (SIF's) calculated from the sum of the elastic thermal stress and the residual stress on the crack plane with effective stress intensity factors deduced from the cracked body analyses. Simple linear summation would normally be expected to yield a conservative estimate of the crack driving force. A value greater than one indicates that simple linear superposition of elastic stress intensity factors is indeed conservative. Figure 7 shows:

- For thermal load acting alone, the elastic SIF is always conservative, and becomes excessively so at high levels of thermal load due to plastic relaxation of stress. This is a well known phenomenon, and procedures such as R6 [1] have means of lessening this conservatism [6].
- For a pre-existing defect, the elastic SIF is non-conservative both for residual stress acting alone (the left-most point in each plot), and up to very high levels of thermal load. This non-conservatism is caused by the plastic residual strain field, which affects J , but is not included in the elastic stress intensity factor calculated from the residual stresses.
- For combined loading of a defect forming after imposition of the residual stress field, the elastic SIF's are generally conservative. This is because the plastic residual strain field does not affect J for this type of defect, making a simple elastic SIF quite a good estimate of the crack driving force due to the residual stress field. There is slight non-conservatism for residual stress alone. This is caused by elastic follow-up, which is discussed below.

Spherical shell

Figure 8 compares the values of the J -integral obtained for simultaneous and progressive opening of the ring defect at a repair weld. Results are plotted for models consisting both of all-weld material and mis-matched weld and casting material. The results for the all-weld model show a marked reduction in J for a defect that opens progressively to the final crack tip. The results for the weld/casting model show that this reduction is more marked if the crack is opened after imposition of the pressure stress.

IMPLICATIONS

There is a clear ranking of J for the different methods of introducing a crack into a residual stress field. The highest value of J is predicted if the crack is assumed to be present prior to imposition of the residual stress field. An intermediate value of J is predicted for a defect that forms after imposition of the residual stress field and opens simultaneously at all nodes. The lowest value of J is predicted for a defect that forms after imposition of the residual stress field and opens progressively to its tip. Which defect model is most relevant to the assessment of real defects?

The results for a pre-existing defect are at first sight somewhat disturbing, since they appear to show that it is unconservative to follow the usual practice of estimating the crack driving force due to a residual stress field from the stress field alone. However, it must be remembered that the residual plastic strain fields of

this study are not necessarily representative of those in a real weld, since they were constructed only to produce representative stress fields, not to reproduce the strain history near a multi-pass weld. Indeed the strain history at a real weld is likely to be cyclic and to include significant unloading, which will make the J-integral strictly invalid. Also, few assessments are actually made of defects forming during welding, at the size present at the end of the welding process: it is much more common to determine a limiting defect size to ensure that there is sufficient margin for sub-critical crack growth. Even if an assessment of the load margin is made at the actual defect size, this size is likely to include a margin for inspection sizing errors, so the assessed defect will be larger than the actual defect in the structure. In both these cases the assessed defect size includes a margin for crack growth, so the crack tip will have propagated beyond the original crack tip damaged zone. The process of defect formation will also act to relax the stresses and strains in the weld. The pre-existing defect results should not therefore be considered representative of real defects at welds.

In contrast, the results for a defect that opens simultaneously to its tip after welding is complete indicate that, for this type of defect, the simple approach of calculating the crack driving force due to a weld residual stress from the uncracked body elastic stress field is quite accurate. Figure 7 shows that this approach agrees with cracked body results within 3% for the less severe residual stress field applied to a defect in a cylinder. Agreement is less good for the more severe residual stress distribution (Figure 7), where the defect is embedded within a region of yield magnitude residual stresses and the elastic SIF is only 84% of the cracked-body results. This under-prediction of crack driving force is due to elastic follow-up in the structure [1]. The simplified assessment of combined residual, thermal and primary loads applied to simultaneously appearing defects is discussed further in [10] and [11], which develop methods for combining weld residual and thermal loads that together produce elastic stresses in excess of yield within the R6 framework.

It is common for real defects to grow by some sub-critical mechanism. For instance, if an estimate is made of the limiting defect size, then the assessed defect includes a margin for sub-critical crack growth. The results for a defect that opens progressively to its tip, which in effect simulates sub-critical crack growth, suggest that the crack driving force is substantially reduced compared with simultaneous opening of the crack flanks (Figure 8). This effect occurs because the growing crack front leaves a plastic wake along its flanks, and a logarithmic strain singularity at the crack tip associated with a moving crack prevails [14]. In contrast, for simultaneous opening the plastic zone is concentrated at the final position of the stationary crack, where a $1/r$ strain singularity at a distance r from the crack tip dominates in a perfectly plastic material. The analyses showed acceptable path independence of J and good correlation between J and the crack tip opening displacement, indicating that the J-integral was providing a measure of the intensity of deformation at the crack tip. It is tempting therefore to conclude that there is considerable pessimism in assessment methods based on simultaneous opening of the crack flanks if these are applied to defects that advance by sub-critical mechanisms. However, the validity of comparing J-integral results computed under these conditions with J-resistance data from standard material property tests is not clear, so these results should be treated with caution (see [4] for more detailed discussion). They do however suggest that there may be considerable pessimism in assessment routes based on defects that open simultaneously [10, 11].

CONCLUSIONS

1. If non-linear cracked body finite element analysis is used to estimate the crack driving force for a defect in a weld residual stress field via the J-integral, then the results depend strongly on the way the defect is introduced into the mesh.
2. In this study the highest value of the J-integral is obtained for a pre-existing defect, since this responds to both the residual stress field and the plastic strain history associated with its imposition.
3. The J-integral for a defect that is introduced after formation of the residual stresses by simultaneous release of the crack flank nodes is lower than that for a pre-existing defect, and agrees well with simplified assessments based on the uncracked-body residual stress field.
4. The lowest value of the J-integral is predicted for a defect introduced after formation of the residual stresses by progressive release of the crack flank nodes. However, it is not clear whether the value calculated has any general validity.

5. The most appropriate method for comparison with real defects is considered to be a defect introduced after formation of the residual stress field by simultaneous release of the crack flank nodes. However, it must be remembered that this approach implicitly assumes that some sub-critical crack growth has occurred.

REFERENCES

- [1] *R6: Assessment of the Integrity of Structures Containing Defects*, R/H/R6 Rev. 3, Amendment 10, British Energy Generation Ltd, Gloucester, May 1999.
- [2] *Guide on methods for assessing the acceptability of flaws in fusion welded structures*, BS 7910:1999, BSI, London, 1999.
- [3] *Structural Integrity Assessment Procedures for European Industry – Final Procedure*, Brite-Euram Project BE95-1426, November 1999.
- [4] P J Bouchard, M R Goldthorpe and P Prottey, J-integral and Local Damage Fracture Analyses for a LWR Pump Casing Containing Large Weld Repairs, to be published in *Int. J. Pres. Ves. & Piping*.
- [5] P Dong, J Zhang and M V Li (1998), Computational modelling of weld residual stresses and distortions – an integrated framework and industrial applications, PVP-Vol. 373, ASME, pp311-317.
- [6] D G Hooton and P J Budden (1995), R6 developments in the treatment of secondary stresses, PVP-Vol. 304, ASME, pp503-509.
- [7] J K Sharples, C C France and R A Ainsworth (1999), Experimental validation of R6 treatment of residual stresses, PVP-Vol. 392, ASME, pp225-238.
- [8] M C Smith, A H Sherry, J Schofield, R Phaal and I C Howard (1998), A comparison of different failure assessment methodologies applied to the NESC-1 test, PVP-Vol. 362, ASME, pp281-287.
- [9] J R Rice (1968), A path independent integral and the approximate analysis of strain concentrations by notches and cracks, *Trans. ASME, J. Applied Mech.*, **35**, pp379-386.
- [10] M C Smith and M R Goldthorpe (2000), The treatment of combined residual and thermal stresses in defect assessments – part 1, zero primary load, ASME Pressure Vessels and Piping Conference, Seattle, July 2000.
- [11] M C Smith and M R Goldthorpe (2000), The treatment of combined residual and thermal stresses in defect assessments – part 2, with additional primary load, ASME Pressure Vessels and Piping Conference, Seattle, July 2000.
- [12] *ABAQUS/Standard User's Manuals*, Version 5.8, Hibbitt, Karlsson and Sorenson Inc., 1080 Main Street, Pawtucket, Rhode Island, USA, 1998.
- [13] P Delfin, I Sattari-Far, and B Brickstad (1998), Effect of thermal and weld-induced residual stresses on CTOD and J-integral in elastic-plastic fracture analysis, Proc. 4th Int. Conf. on Engineering Structural Integrity Assessment.
- [14] J R Rice, W J Drugan, and T L Sham (1980), Elastic-plastic analysis of growing cracks, *Frac. Mech. 12th Conf. ASTM STP 700*, pp189-221.

APPENDIX: DEFINITION OF SECONDARY REFERENCE STRESS

A non-dimensional parameter R is used to quantify the magnitude of the secondary stress fields. R relates the magnitude of combined secondary reference stress, σ^s , to the 0.2% proof stress and is defined as follows:

$$R = \sigma^s / \sigma_{0.2}$$

where the combined secondary reference stress, σ^s , is given by:

$$\sigma^s = \sigma^{\text{res}} + \sigma^{\text{th}}$$

The two components, σ^{res} and σ^{th} , are determined as follows:

$$\sigma^{\text{res}} = K_I^{s,\text{res}} / Y \sqrt{\pi a}$$

and

$$\sigma^{th} = K_I^{s,th} / Y \sqrt{\pi a}$$

where $K_I^{s,res}$ is the elastic stress intensity factor due to a nominal stress distribution equal to the elastic-plastic field of uncracked residual stress acting alone and $K_I^{s,th}$ is the actual elastic stress intensity factor due to the thermal load acting alone. Y is the non-dimensional stress intensity function due to a uniform tensile axial stress, σ^p , and is given by:

$$Y = K_I^p / \sigma^p \sqrt{\pi a}$$

where K_I^p is the appropriate stress intensity factor.

FIGURES

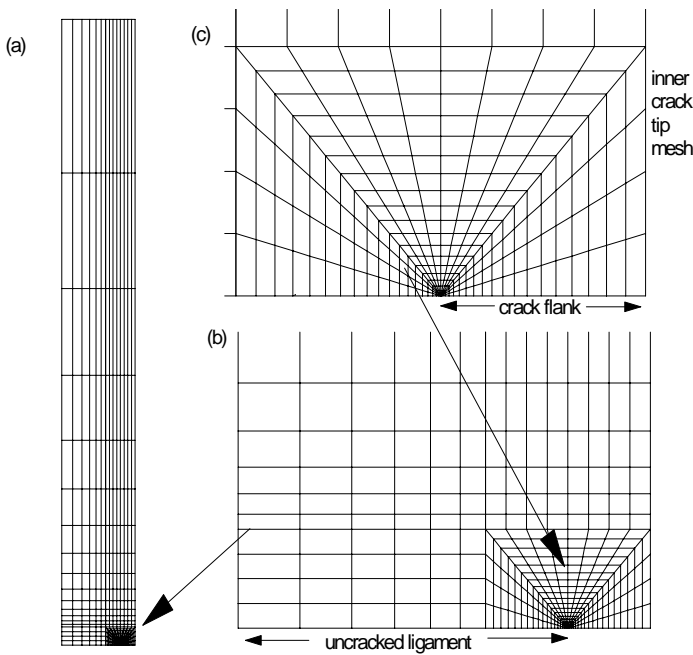


FIGURE 1: FINITE ELEMENT MESH FOR CIRCUMFERENTIALLY CRACKED CYLINDER

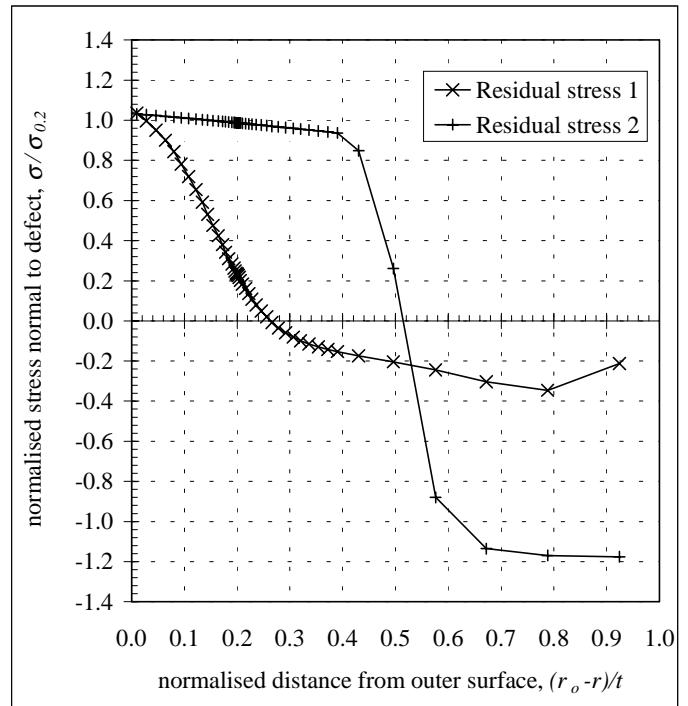


FIGURE 2: RESIDUAL STRESS FIELDS IN CIRCUMFERENTIALLY CRACKED CYLINDER

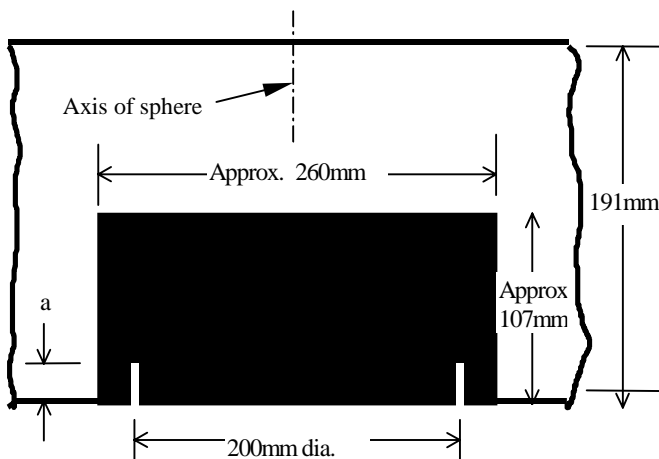


FIGURE 3: DETAILS OF REPAIR WELD AND "RING" DEFECT AT NORTH POLE OF SPHERE

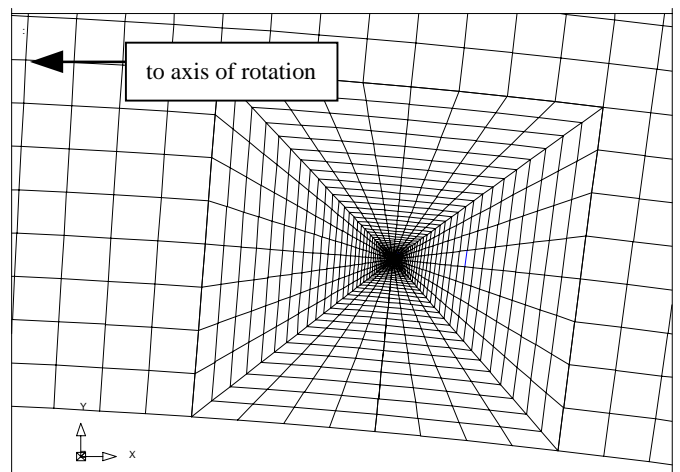


FIGURE 4: CRACK TIP REGION OF "RING" DEFECT IN SPHERE

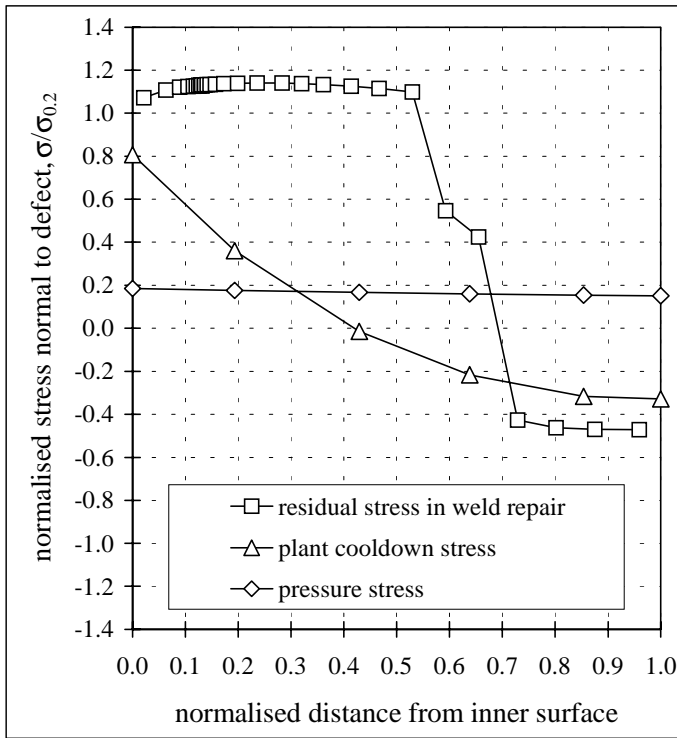


FIGURE 5: RESIDUAL STRESS FIELD AND ELASTIC APPLIED STRESSES FOR REPAIR WELD DEFECT IN SPHERE

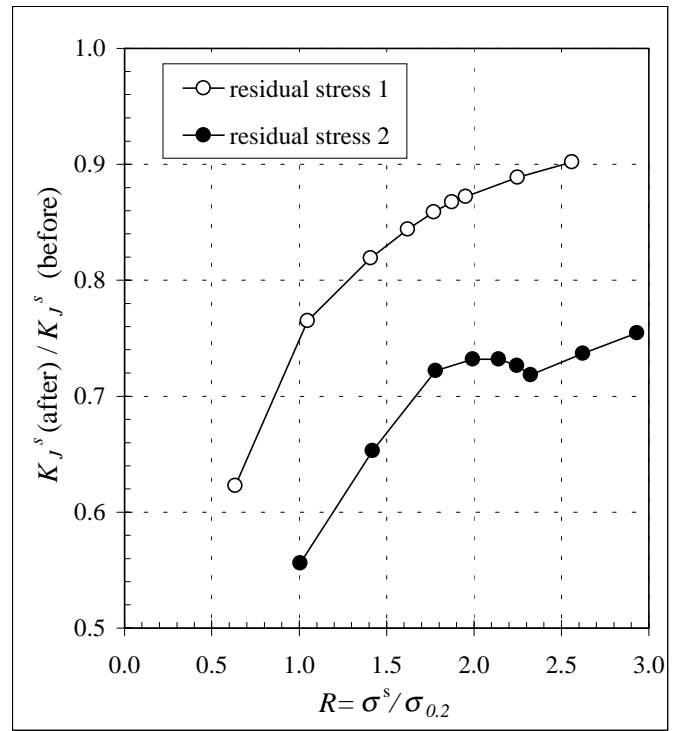


FIGURE 6: RATIO OF THE EFFECTIVE STRESS INTENSITY FACTOR FOR A DEFECT INTRODUCED AFTER IMPOSITION OF THE RESIDUAL STRESS FIELD TO THAT FOR A PRE-EXISTING DEFECT IN A CYLINDER

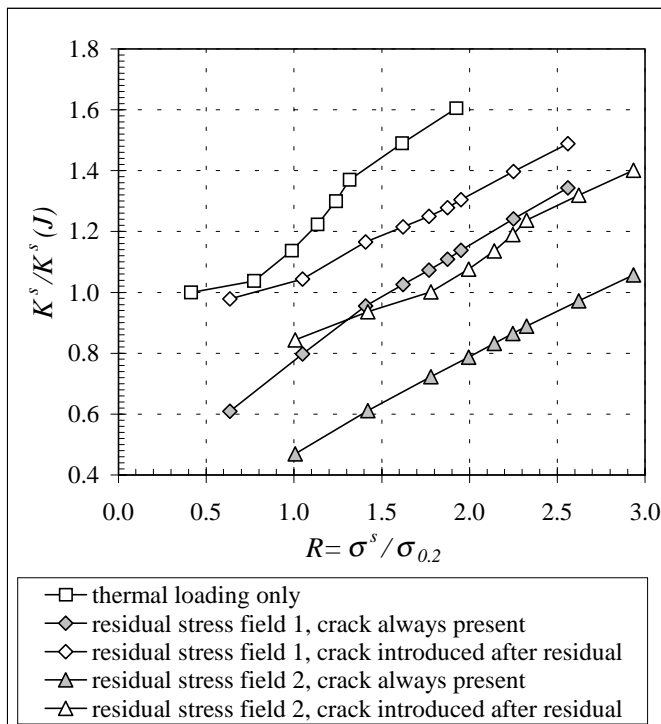


FIGURE 7: RATIO OF THE ELASTIC SIF TO THE EFFECTIVE STRESS INTENSITY FACTOR DEDUCED FROM THE J-INTEGRAL FOR A DEFECT IN A CYLINDER

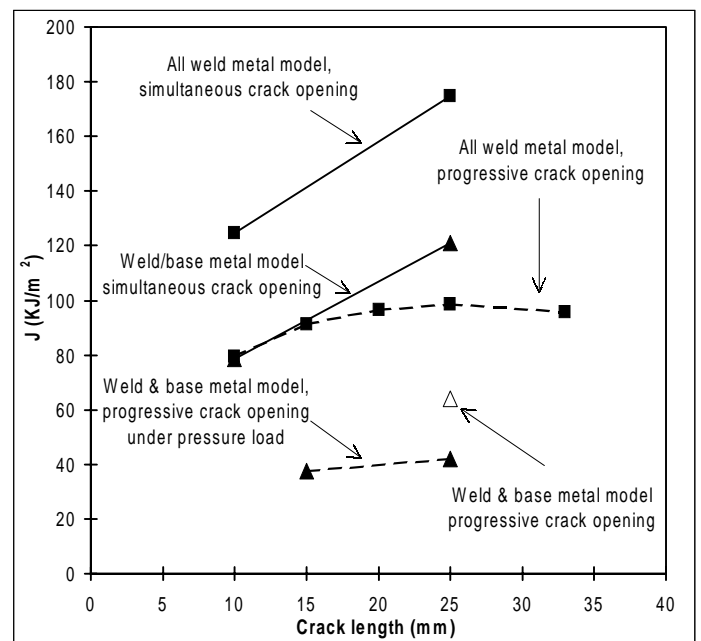


FIGURE 8: J-INTEGRAL PREDICTIONS UNDER RESIDUAL, PRESSURE, AND THERMAL LOADS FOR A "RING" DEFECT AT A REPAIR WELD IN A SPHERE